MMC FOR GRID CONNECTED PV SYSTEM TO IMPROVE THE POWER QUALITY UNDER PARTIAL SHADING CONDITIONS

V. Venkateswara Rao[1], Ch. Rami Reddy[2], G. Rami Reddy[3]

[1,2,3] Department of Electrical and Electronics Engineering, Nalanda Institute of Engineering Technology, Guntur, Andhra Pradesh, India. crreddy229@gmail.com, dr.g.ramireddy76@gmail.com

ABSTRACT: Photovoltaic (PV) energy generation is becoming an increasingly widespread means of producing clean and renewable power. In PV systems, long strings of photovoltaic modules are found to be vulnerable to shading effects, causing significant reduction in the system power output. In the case of partial shading, the output power of the unshaded PV modules will be decreased by the influence of the shaded PV modules in one branch. In order to solve this problem, this paper proposes a novel topology for a PV power generation system by connecting a PV module to the capacitor in each sub module of a modular multilevel converter parallel. As partial shading occurs, the maximum power can be extracted by regulating the capacitor voltage to the maximum power point voltage. With this proposed topology, the maximum power tracking controller, the redundancy module controller, the voltage stability controller, and the grid-connected controller are studied. Simulation and experiment results show that comparing to the traditional topology; the proposed topology can greatly improve the output power of the PV system under the conditions of partial shading and features with low-voltage stress and high efficiency. Matlab/simulink simulations are presented in order to show the outstanding performance of the proposed design approach.

I. INTRODUCTION

As the time a progress, the demand of power is increasing gradually and on the contrary the fossil fuels used for power generation are decreasing rapidly. Alongside the reason of inadequate resources, the methods that are used for power generation by fossil fuels are not even eco-friendly and they are causing global warming and greenhouse effects. Now would be the proper time to initiate the usage of renewable energy resources on very large scale. The renewable energy resources that are available to us are Solar Energy, Hydro Energy and Wind Energy. They are rich in quantity, pollution free, distributed all through the earth and recyclable [1-5]. Hydro Energy generation, Wind Energy generation are of course two of the main sources of renewable energies, but the disadvantage in Hydro Energy is that, it is seasonal dependent and in Wind energy is that it depends on geographical location. On the contrary, Solar Energy is widespread all over the globe and all the time. Also most of the remote areas have not been connected to the grid and they do not have power supply. These areas can generate power on their own using renewable resources such as solar energy. The amount of irradiance and temperature vary from location to location and from time to time but under given conditions Solar Energy system can be installed [6-15].

Photo Voltaic energy system is the most direct way to convert the solar radiation into electricity based on photovoltaic effect. Despite high initial costs, they have already been implemented in many areas. Research is going into this area to develop the efficient control mechanism and provide better control. Recent developments in the technology of batteries and solar panel efficiencies offer a better performance. So the overall installation cost of photovoltaic charging system reduces. And therefore, the time is not so far that almost any and every middle class person can afford a solar panel at home for at least some basic requirements. In the light of above points, it is clear that Solar Energy plays an important role in the forthcoming future. So, it is our duty to learn, implement and improvise the idea as early as possible, so that it becomes a very useful tool to our future generations [16-23].

II. SYSTEM MODELING

The proposed topology of the PV power generation system is shown in Fig. 1. Comparing to the traditional MMC circuit used in the PV system, the proposed one removes the long string PV modules connected to the dc side of the MMC, and connects a PV module to the capacitor of each sub module of the MMC in parallel. Because no PV modules are connected in series, the bypass diodes are also removed. When there is partial shading, the maximum power can be extracted by regulating the capacitor voltage in each PM to VMPP. The voltage of the capacitor in the PM may fluctuate according to the irradiance. Although the voltage fluctuation is insignificant for a single module, it could not be neglected when a large number of PMs are connected in series. Therefore, a redundant module (RM) is designed to compensate the voltage loss. The one phase equivalent circuit of the novel topology is shown in Fig. 1(b).

The operation states of PM are summarized as follows.

State I: T1 is switched ON and T2 is switched OFF, the terminal voltage of PM equals to the capacitor voltage UPV.

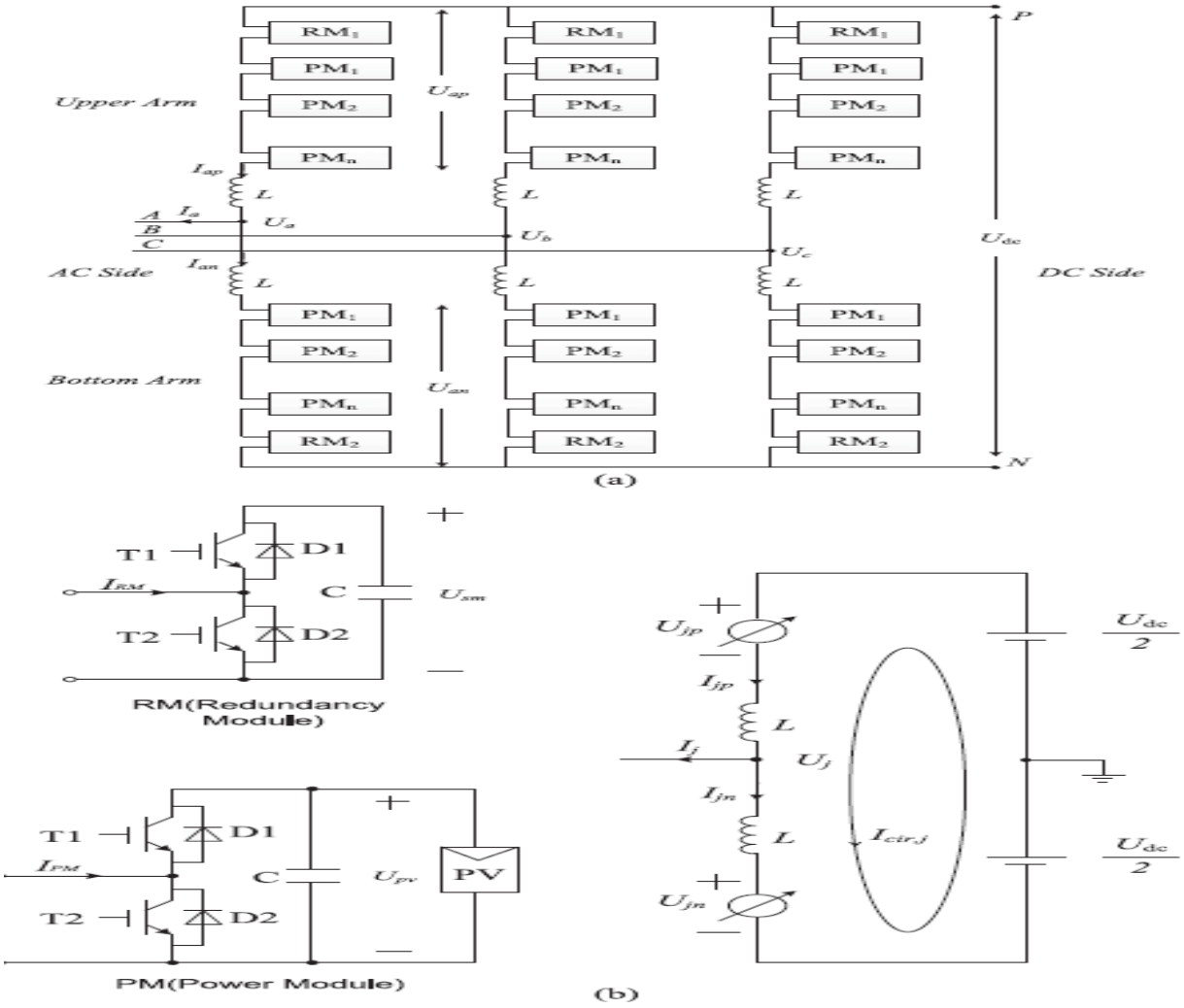

Fig: 1. Novel topology of the PV power generation system. (a) Topology. (b) One-phase equivalent circuit

State II: T1 is switched OFF and T2 is switched ON, the terminal voltage of PM is 0.
State III: T1 is switched OFF and T2 is switched OFF, the terminal voltage of PM is uncertain.
The PM's capacitor voltages under different operation states are described as follows:
1) State I: The variation of the PM's capacitor voltage ΔUPV can be expressed by under this state.

$$\Delta U_{\mathrm{PV}} = \frac{1}{C}\int (i_{\mathrm{PV}} - i_{\mathrm{PM}})dt$$

where i_{PV} is the output current of the PV module, i_{PM} is the output current of the PM, and C is the value of the capacitor in each PM. If the current iPM flows into the PM from the midpoint, as shown in Fig. 2(a), the capacitor will be charged by iPM and iPV. Then, the capacitor voltage UPV will rise quickly. Oppositely, if iPM flows out from the PM, UPV will drop when iPM > iPV, as shown in Fig. 2(b), and rise when iPM < iPV as shown in Fig. 2(c).

2) State II: ΔUPV is expressed as below under this state

$$\Delta U_{\mathrm{PV}} = \frac{1}{C}\int i_{\mathrm{PV}}\,dt.$$

The capacitor is charged by iPV, and its voltage UPV rises regardless of the direction of iPM, as shown in Fig. 2(d) and (e).

3) State III: ΔUPV is expressed by under this state

$$\Delta U_{\mathrm{PV}} = \frac{1}{C}\int (S(i_{\mathrm{PM}}) + i_{\mathrm{PV}})dt$$

where "S()" is a function of I'PM, when iPM ≥ 0, its output is i_{PM}, otherwise, its output is 0. If iPM flows into the PM, as shown in Fig. 2(f), UPV will be charged by iPM and iPV together. As a result, it will rise quickly. Oppositely, if iPM flows out from the PM, as shown in Fig. 2(g), UP V will also rise because it is charged by iPV. From the above analyses, the capacitor voltage UPV can be controlled to be the MPP voltage of PV module by choosing suitable working

states in according to the direction of iPM. Table I shows the relationships of working states, direction of iPM, and changing trend of UPV. Here, "1" denotes switching on, "0" denotes switching off. Taking phase A as an example, the block diagram of the control method is shown in Fig. 3, which is divided into four parts: I) the maximum power tracking controller, 2) the redundancy module controller, 3) the voltage stability controller, and 4) the grid-connected controller.

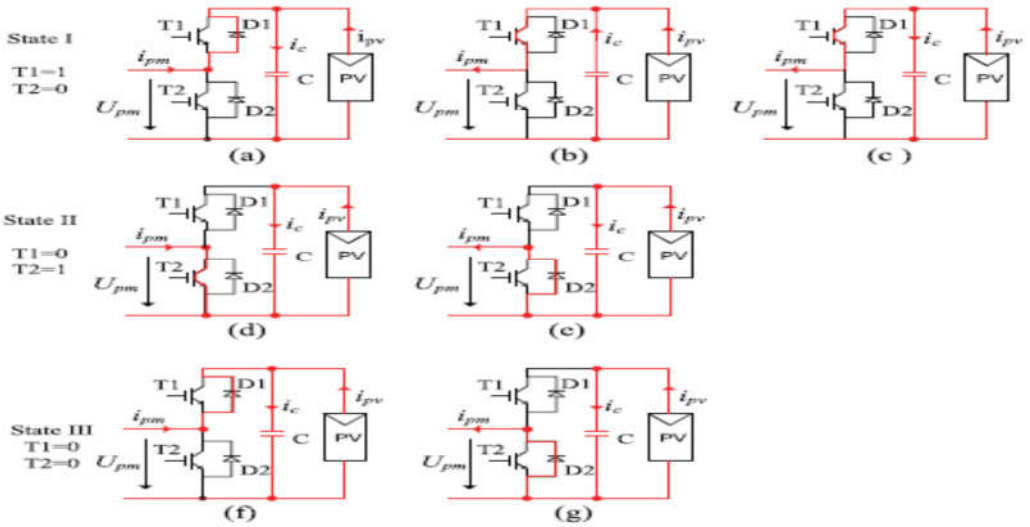

Fig: 2. Working states of PM

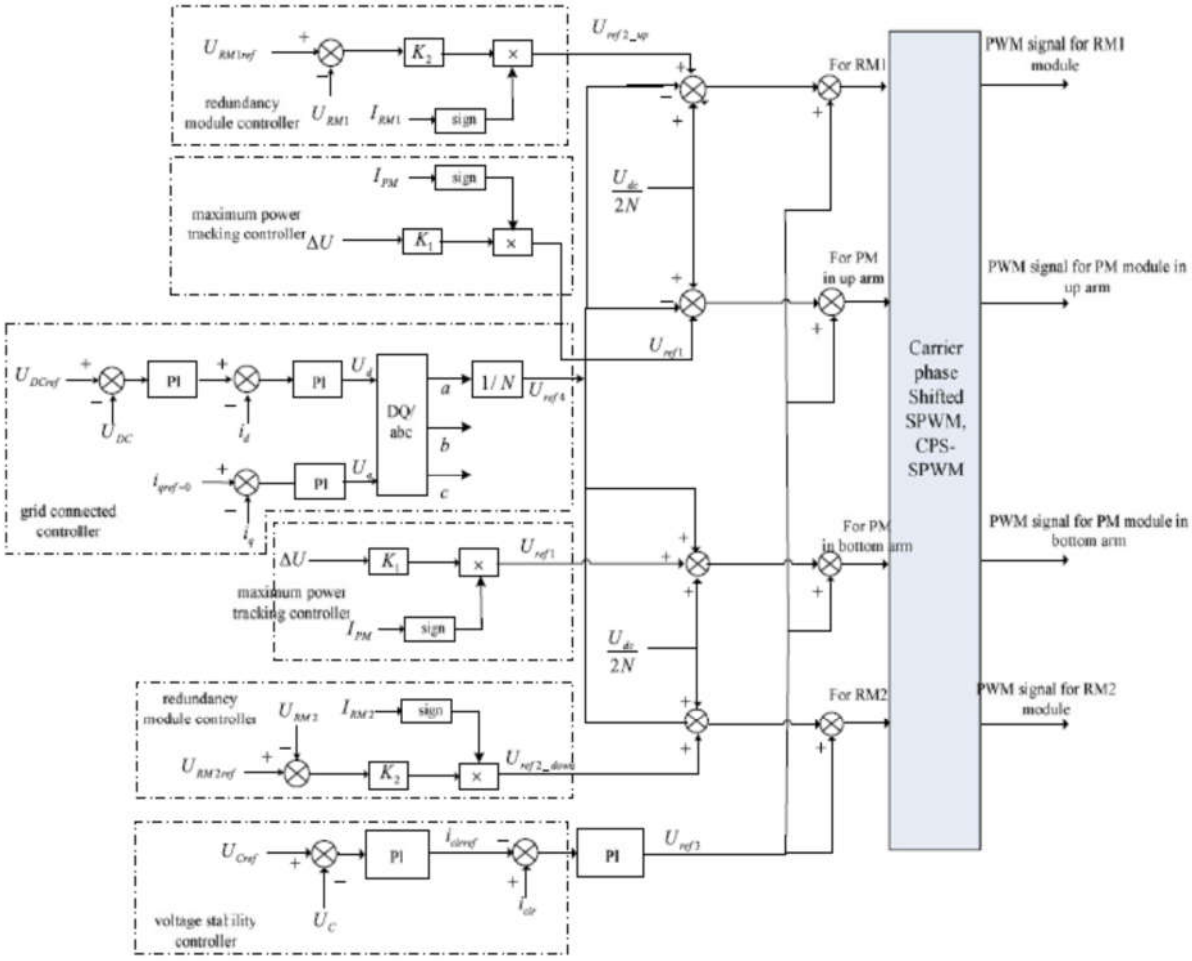

Fig: 3. Block diagram of the control method.

The outputs of these controllers are Uref1, Uref2, Uref3, and Uref4, respectively. The grid-connected controller gets the main modulation waveform Uref4, and its purpose is to achieve the energy delivery from PV module to power grid. The voltage stability controller is used to balance the voltages between phases. The modulation waveform Uref3 generated by the voltage stability controller is superimposed on the main modulation waveform, which will change the output power of each phase. Through this adjustment, the voltage balance of phases can be realized. The redundancy module controller is used to regulate the voltage of capacitor in RM. Its output modulation waveform Uref2 is superimposed on the main modulation waveform too, which can change the charge and discharge time of the capacitor in RM. The maximum power tracking controller is used to obtain MPP voltage of the PV module. Its working principle is like that of redundancy module controller. When the PV modules work at the MPP, the voltages of capacitors in PMs may be unequal, but the difference is small, which will have a little influence on the THD of the output current of the topology.

IV. SIMULATION RESULTS

Case: 1- Partial shading With the Proposed Topology and Control Method

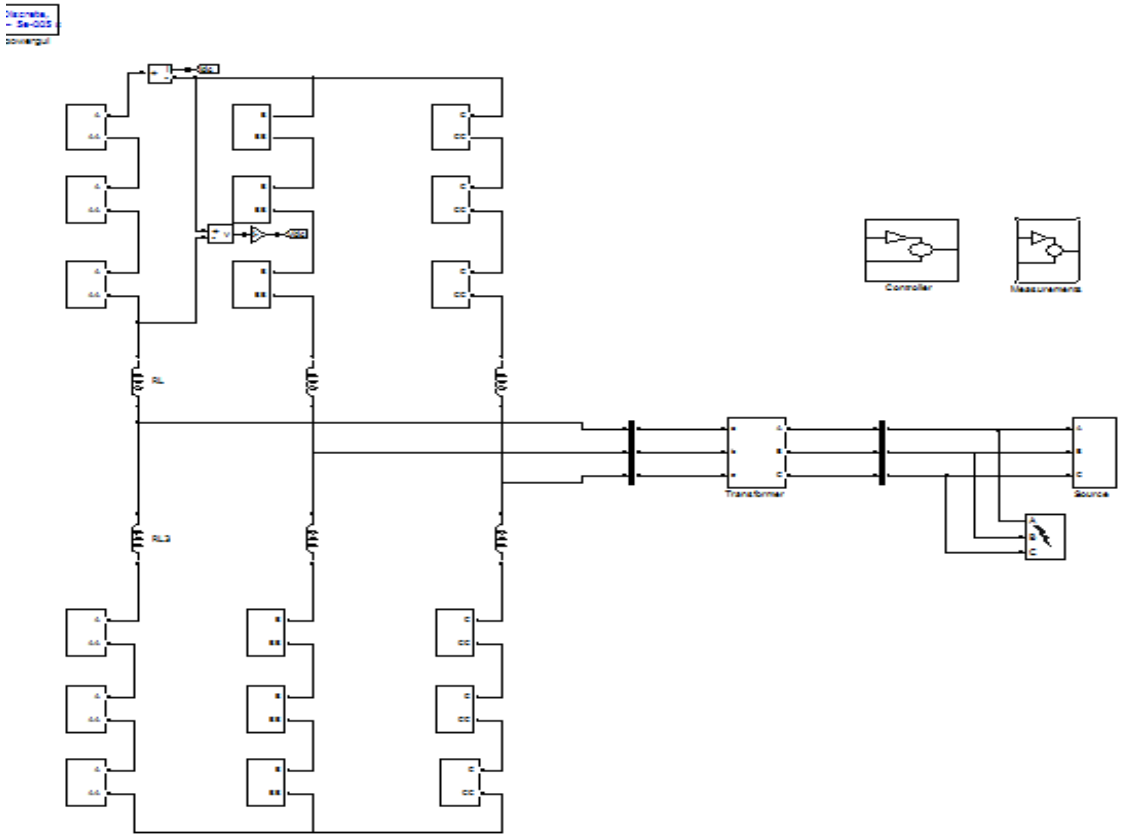

Fig: 4. simulation diagram of Partial shading With the Proposed Topology and Control Method

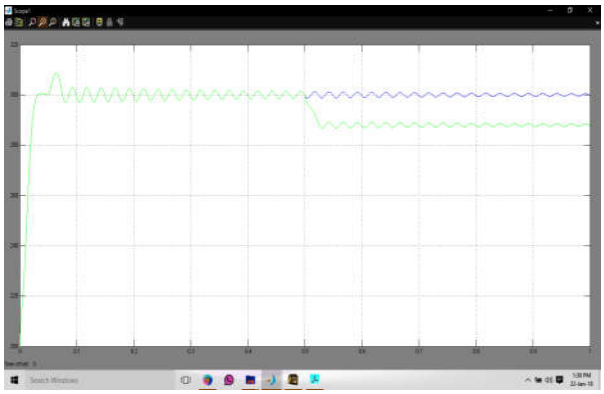

Fig: 5(a)

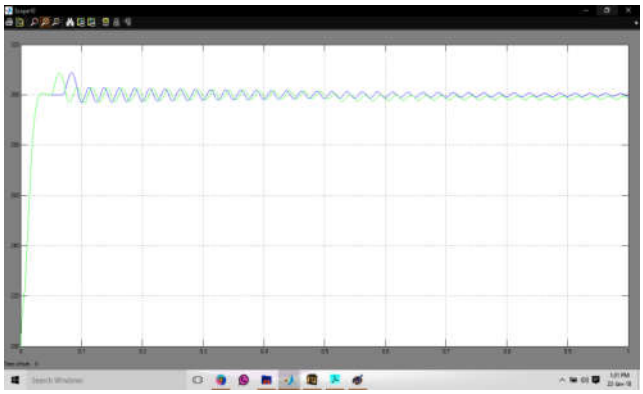

Fig:5(b)

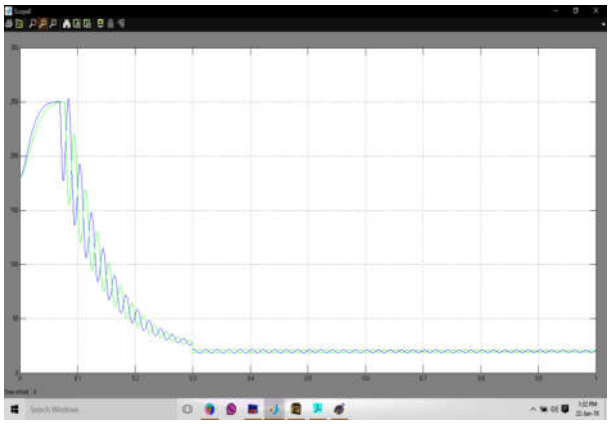

Fig: 5(c)

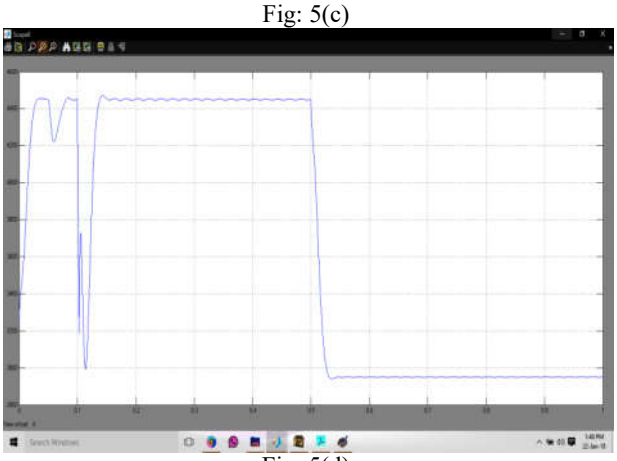

Fig: 5(d)

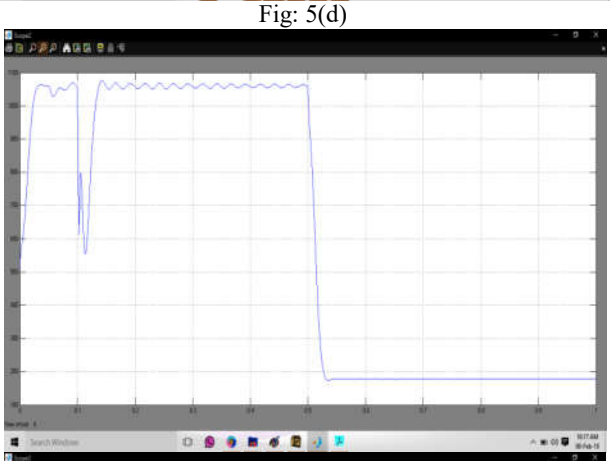

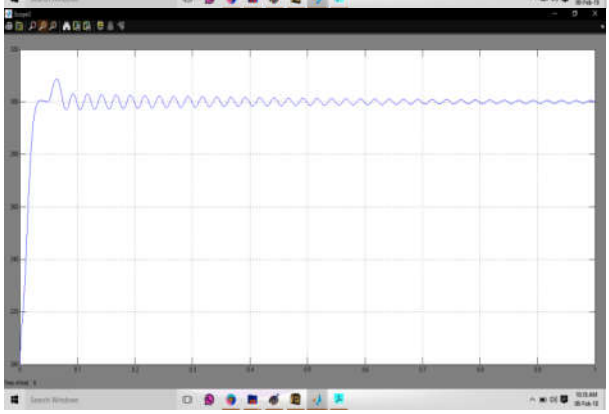

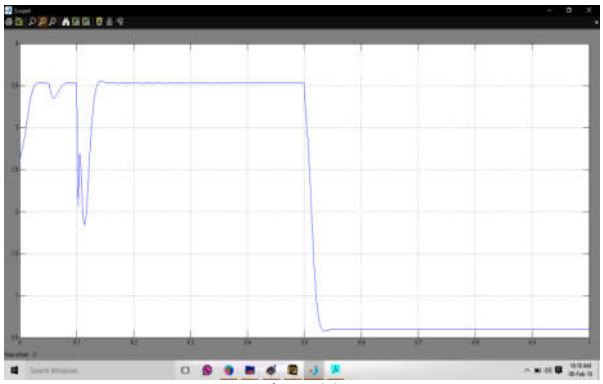

Fig: 5(e)

Fig: 5. Voltage and power waveforms under partial shading. (a) Capacitor voltages of PM1 and PM2. (b) Capacitor voltages of PM3 and PM4. (c) Capacitor voltages of RM1 and RM2. (d) Output power waveform. (e) Output waveforms of PV1 module in PM.

In this case, the irradiance of all PMs is set to 1000 W/m2 initially. After 0.5 s, the irradiance is changed to 200, 800, 400, and 1000 W/m2, respectively. The simulation results are shown in Fig. 5. Fig. 5(a) shows the capacitor voltages of two PMs in upper arm of phase A. Both of the voltages are about 300 V initially, and then change to 278 and 300 V with a ripple of about 6 V, respectively. Because the output power of the PV module is closely related to its output voltage, the ripple of capacitor voltage of PM will decrease the output power of PV module. The capacitance value of PM needs to be increased to reduce this voltage ripple. According to the *P–U* characteristics of the PV module, it is known that within a short range near the MPP, the change of output voltage has a little effect on the output power of the PV module. Therefore, this paper selects the capacitance to be 2000 μF, and with this capacitance value, the voltage ripple is reduced to be less than 3%, the power loss is less than 1%. Fig. 5(b) shows the capacitor voltages of two PMs in the bottom arm. The voltages change from 300 to 292 V and 302 V, respectively, which is caused by the MPPT controller. It is known that all PV modules still operate at their MPP even under partial shading. Fig. 5(c) shows the capacitor voltages of two RMs. The value is near 0 V initially, and that means the redundancy modules do not work under no shading conditions. After 0.5 s, the capacitor voltages of RM1 and RM2 increase to 14, 5 V, respectively. It means that the redundancy module can compensate the voltage loss which is caused by partial shading. Fig. 5(d) shows the output power waveform of phase A. Its value is about 4400W before 0.5 s and 2585Wafter 0.5 s. This value is very close to the theoretical value, 2602 W, which can be calculated. Fig. 5(e) shows the output waveforms of the PV module in PM1. The output current is 3.65 A initially, and then drops to 0.56 A immediately at 0.5 s for the irradiance changing to 200 W/m2. With the adjustment of MPPT controller, the current come back to 0.65Aat 0.52 s. The output power is dropped from 1106 to 170Wat 0.5 s and come back to 192Wat 0.52 s. These results are very close to the theoretical value which justifies the effectiveness of the MPPT controller. Note that the voltage reference of RMs is 0 V before 0.5 s, but the capacitor voltages of RMs cannot be a negative

value. Hence, during the discharge process, the capacitor voltages of the RMs could only be reduced to 0 V, and during the charging process, the capacitor voltages start to rise. In view of the overall process, the average value of the capacitor voltage has an offset from zero. The offset is not big, and its influence can be ignored. Furthermore, when the RMs need to contribute a big voltage compensation, the offset will disappear automatically.

Case: 2- Some PM is Burnt Out Suddenly

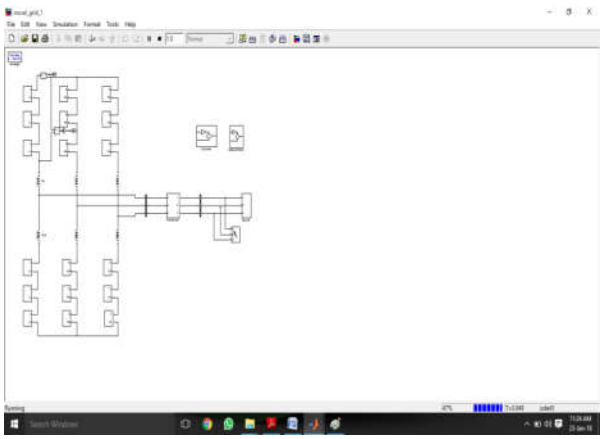

Fig: 6. simulation diagram of Some PM is Burnt Out Suddenly

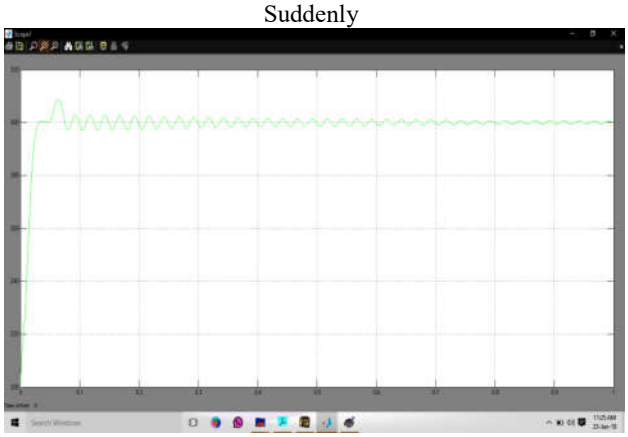

Fig: 7(a)

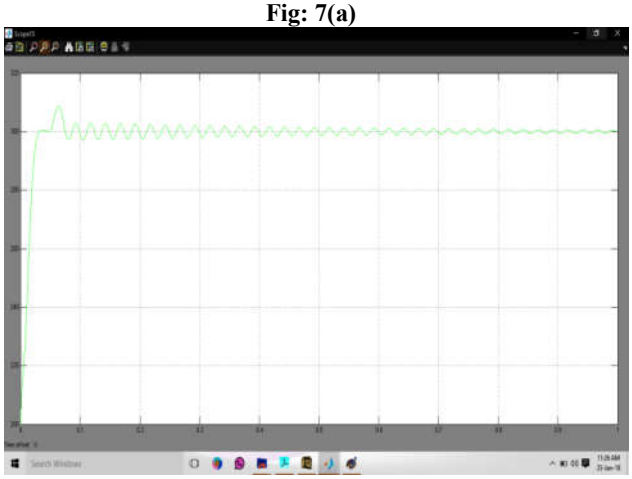

Fig: 7(b)

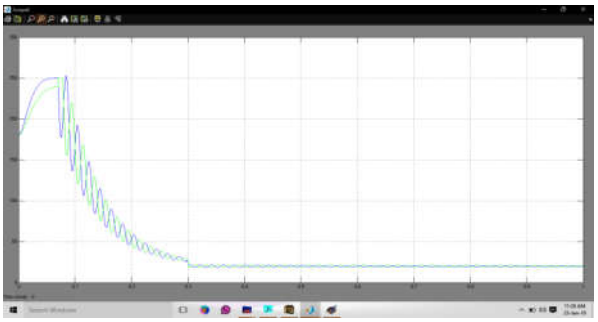

Fig: 7(c)

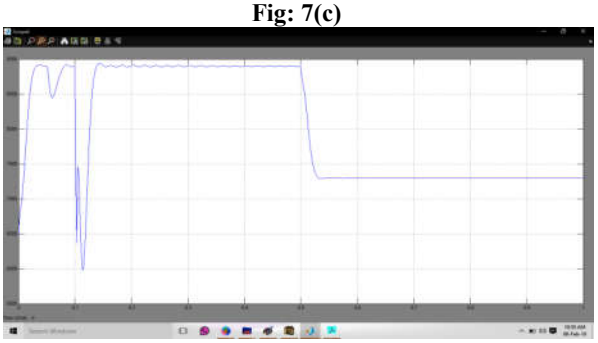

Fig: 7(d)

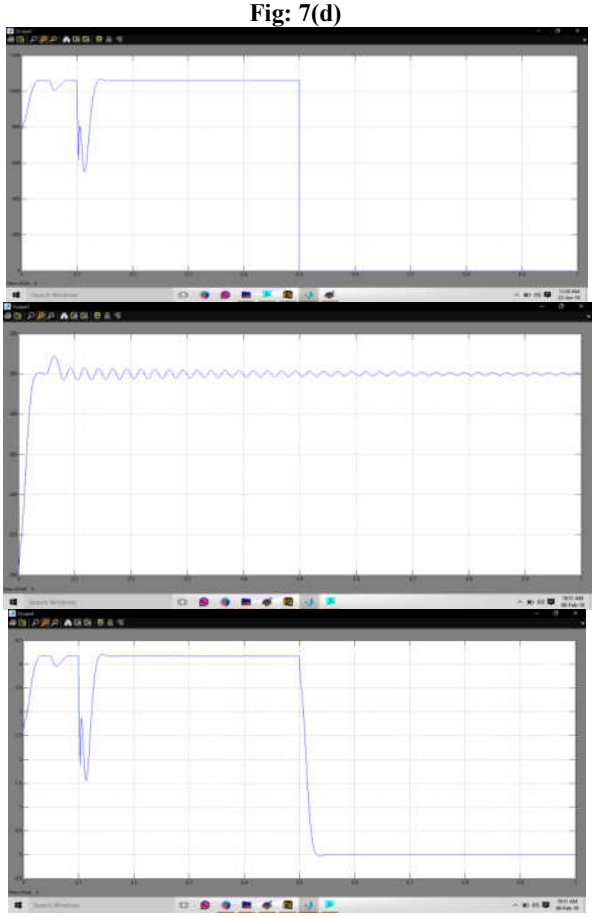

Fig: 7(e)

Fig: 7. Voltage and power waveforms when PM1 is burnt out. (a) Capacitor voltages ofPM1and PM2. (b) Capacitor voltages of PM3 and PM4. (c) Capacitor voltages of RM1 and RM2. (d) Output power waveform. (e) Output waveforms of PV module in PM1.

In this case, the irradiance of all PMs of phase A is set to 1000 W/m2 initially. After 0.5 s, the PV module in PM1 is burnt out, and the output current of this PV module drops to zero immediately. The simulation results are shown in Fig. 7. Fig. 7(a) and (b) are the capacitor voltages of PMs in upper arm and bottom arm, respectively. The voltage of capacitor in each PM is about 300 V before 0.5 s, which means that all PV modules work at their MPP. After 0.5 s, the capacitor voltage of PM1 is slightly decreased to 294 V, and then goes back up to300 V at 0.6 s. However, the other PMs still work at their MPP, keeping the capacitor voltages at 300 V. Fig. 7(c) shows the capacitor voltages of RM modules. The capacitor voltages of RM1 and RM2 are near 0 V all the time. It is because that when any PV module is burnt out, the corresponding PM works as a RM. So theoretically speaking, the voltage loss can be compensated no matter how many PMs are burnt out. Fig. 7(d) shows the output power. The value is about 4400W before 0.5 s and 3300 W after 0.5 s. Fig. 7(e) shows the output waveforms of the PV module in PM1. The current is 3.6A before 0.5 s, and then drops to zero immediately for the reason that the PV module is burnt out, and the output power is dropped from 1106 W to 0 immediately too. These simulation results consist with the theoretical analysis well.

Case: 3- Reconfigure Structure under Partial Shading

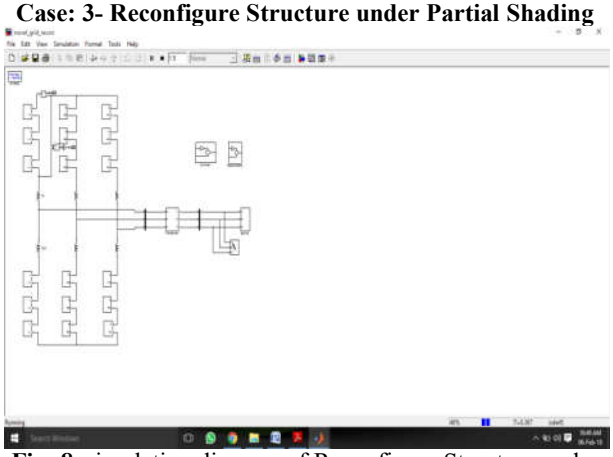

Fig: 8. simulation diagram of Reconfigure Structure under Partial Shading

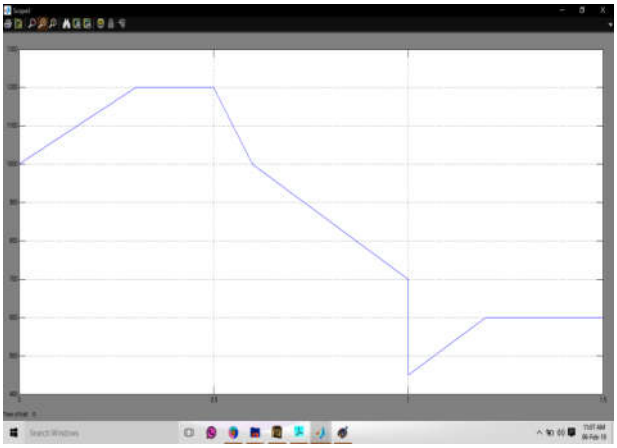

Fig: 9(a)

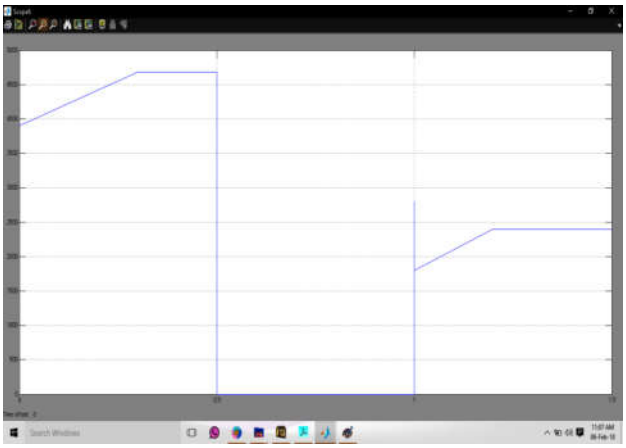

Fig: 9(b)

Fig: 9. Power and voltage waveforms with reconfigure structure under partial shading. (a) Output power. (b) Output voltage of PV array.

So, the global MPPT will be easier to realize. The output power is about 4400 W initially, and suddenly drops to 0 W, which is because that the structure of PV array is reconfigured, and the terminal voltage of PV array exceeds its open-circuit voltage, as shown in Fig. 9(a) clearly. The terminal voltage of PV array is 1195 V before 0.5 s and then decreases to 610 V gradually. That means the MPPT method converges to point B, and the output power of PV array reaches to 2323W, which is more than that of traditional topology, but still less than that of the proposed topology.

V. CONCLUSION

A novel topology for the PV array is proposed, where a PV module is connected to the capacitor of each sub module of MMC in parallel. It aims to improve the output power under partial shading by regulating the voltage of capacitor in each PM to the MPP voltage of PV module. A RM is designed and connected to each bridge arm of the MMC to compensate the voltage loss caused by the irradiance variation. The proposed PV topology has lower voltage stress on switching device and higher efficiency. The control strategy has four parts: 1) the maximum power tracking controller, 2) the redundancy module controller, 3) the voltage stability controller, and 4) the grid-connected controller. Experimental verifications were performed by building a 3-kW PV system experimental platform. Simulation results show that the proposed topology has the same efficiency as that of the traditional topology under no shading, but achieves higher efficiency under partial shading, and compared with the reconfiguration structure, the proposed topology not only eliminates the complexity of the reconfiguration structure, but also achieves the ability of higher output power under partial shading.

REFERENCES

[1]. R. Balasubramanian, S. I. Ganesan, and N. Chilakapati, “Impact of partial shading on the output power of PV systems under partial shading conditions,” IET Power Electron., vol. 7, no. 3, pp. 657–666, 2014.

[2]. K. Chen et al., "An improved MPPT controller for photovoltaic system under partial shading condition," IEEE Trans. Sustainable Energy, vol. 5, no. 3, pp. 978–985, Jun. 2014.

[3]. Ch Rami Reddy, K Harinadha Reddy "Islanding Detection using DQ Transformation based PI Approach in Integrated Distributed Generation", International Journal of Control Theory and Applications, volume: 10, issue: 5, pp. 679-690, 2017

[4]. Ch. Rami Reddy, K. Harinadha Reddy "A passive islanding detection method for neutral point clamped multilevel inverter based distributed generation using rate of change of frequency analysis", International Journal of Electrical and Computer Engineering, volume: 08, issue: 04, pp: 1967-1976, 2018.

[5]. M. Z. S. El-Dein, M. Kazerani, and M. M. A. Salama, "Optimal photovoltaic array reconfiguration to reduce partial shading losses," IEEE Trans. Sustainable Energy, vol. 4, no. 1, pp. 145–153, Jan. 2013.

[6]. Ch Rami Reddy, K Harinadha Reddy "Islanding detection method for inverter based distributed generation based on combined changes of ROCOAP and ROCORP", International Journal of Pure and Applied Mathematics, volume: 117, issue: 19, pp: 433-440, 2017.

[7]. Sk. Shameem, Sk. Nazma, Ch. Rami Reddy "Improving Transient Stability of a Distribution Network by using Resonant Fault Current Limiter", International Journal of Innovative Technologies, volume:06, issue:01, pp: 0376-0383, 2018.

[8]. Ch Rami Reddy, K Harinadha Reddy "Recognition of islanding data for multiple distributed generation systems with ROCOF shore up analysis", Smart Intelligent Computing and Applications, volume: 104, pp: 547-558, 2019.

[9]. G Hima Bindu, K Venkata Reddy, Ch. Rami Reddy "Simulation of High Step-Up Resonant Parallel LC Converter for Grid Connected Renewable Energy Sources", International Journal on Recent and Innovation Trends in Computing and Communication, volume: 04, issue: 03, pp: 84-94, 2016.

[10]. A. Qahouq and J. A. Yuncong Jiang, "Distributed photovoltaic solar system architecture with single-power inductor single-power converter and single-sensor single maximum power point tracking controller," IET Power Electron., vol. 7, no. 10, pp. 2600–2609, 2014.

[11]. Ch. Rami Reddy, K. Harinadha Reddy "Islanding detection for inverter based distributed generation with Low frequency current harmonic injection through Q controller and ROCOF analysis", Journal of Electrical Systems, volume: 14, issue: 02, pp: 179-191, 2018.

[12]. O. Anil Kumar, Ch. Rami Reddy "Hybrid Neuro-Fuzzy controller based Adaptive Neuro-Fuzzy Inference System Approach for Multi-Area Load Frequency Control of Interconnected Power System", International Journal of Electrical and Electronics Engineering, volume: 03, issue: 01, pp: 17-25, 2016.

[13]. A Alisson Alencar Freitas et al., "High-voltage gain dc–dc boost converter with coupled inductors for photovoltaic systems," IET Power Electron., vol. 8, no. 10, pp. 1885–1892, 2015.

[14]. K. V. Siva Reddy, SK. Moulali, K. Harinadha Reddy, Ch. Rami Reddy, B. V. Rajanna, G. Venkateswarlu, Ch. Amarendra "Resonance Propagation and Elimination in Integrated and Islanded Micro grids", International Journal of Power Electronics and Drive System, volume:9, issue: 3, pp. 1445-1456, 2018

[15]. Mallikarjun Balasaheb Patil, Ch. Rami Reddy "Fault detection and mitigation in multilevel converter STATCOMS", International Journal of Advanced Technology in Engineering and Science, volume: 03, issue: 01, pp: 343-349, 2015.

[16]. G. Naveen, K. Harinadha Reddy, Ch. Rami Reddy, B. Ramakrishna, P. Bramaramba "Passive islanding detection method for integrated DG system with balanced islanding", International Journal of Pure and Applied Mathematics, volume: 120, issue: 06, pp: 4041-4058, 2018.

[17]. G. Acciari, D. Graci, and A. L. Scala, "Higher PV module efficiency by a novel CBS bypass," IEEE Trans. Power Electron., vol. 26, no. 5, pp. 1333–1336, May 2011.

[18]. Ch. Rami Reddy, K. Harinadha Reddy, Sk. Karimulla, J. Suneel Babu, B. Praveen Kumar, G. Naveen "A novel passive approach for islanding detection of integrated DG system under zero power imbalance", International Journal of Pure and Applied Mathematics, volume: 120, issue: 06, pp: 4059-4077, 2018.

[19]. R. P. Vengatesh and S. E. Rajan, "Investigation of the effects of homogeneous and heterogeneous solar irradiations on multicrystal PV module under various configurations," IET Renew. Power Gener., vol. 9, no. 3, pp. 245–254, 2015.

[20]. A. Bidram, A. Davoudi, and R. S. Balog, "Control and circuit techniques to mitigate partial shading effects in photovoltaic arrays," IEEE J. Photovoltics, vol. 2, no. 4, pp. 532–546, Oct. 2012.

[21]. G. V. V. Nagaraju , G. Sambasiva Rao , Ch. Rami Reddy "Sensor less voltage control of CHB multilevel inverter fed three phase induction motor with one dc source per each phase", International Journal of Pure and Applied Mathematics, volume: 120, issue: 06, pp: 4079-4097, 2018.

[22]. J. D. Bastidas-Rodriguez et al., "Maximum power point tracking architectures for photovoltaic systems in mismatching conditions," IET Power Electron., vol. 7, no. 6, pp. 1396–1413, 2014.

[23]. S. Lyden and Md. E. Haque, "A simulated annealing global maximum power point tracking approach for PV modules under partial shading conditions," IEEE Trans. Power Electron., vol. 31, no. 6, pp. 4171–4181, Jun. 2016.